Contents lists available at ScienceDirect

Engineering Science and Technology, an International Journal

journal homepage: www.elsevier.com/locate/jestch

Full Length Article

Thermal and physico-mechanical stability of recycled high density polyethylene reinforced with oil palm fibres

R.O. Medupin [a,b,d,*], O.K. Abubakre [b,d], A.S. Abdulkareem [c,d], R.A. Muriana [b], I. Kariim [c,d], S.O. Bada [e]

[a] Mechanical Engineering Department, The Federal Polytechnic, P. M. B. 55, Bida, Nigeria
[b] Mechanical Engineering Department, Federal University of Technology, P. M. B. 65, Minna, Nigeria
[c] Chemical Engineering Department, Federal University of Technology, P. M. B. 65, Minna, Nigeria
[d] Nanotechnology Research Group, Centre for Genetic Engineering and Biotechnology, Federal University of Technology, P. M. B. 65, Minna, Nigeria
[e] Clean Coal Technology Group, School of Chemical and Metallurgy, University of the Witwatersrand, Johannesburg, South Africa

ABSTRACT

The impressive physical and mechanical properties achievable with organic fillers make them a good choice for polymer composite reinforcement. In this study, oil palm fibres (OPF), often hardly thought of as having any reasonable economic value in developing economy was used as reinforcing fillers in recycled high density polyethylene (rHDPE). Thermal behaviour, physical and mechanical stability of rHDPE filled with OPF have been studied. Fourier Transform Infrared Spectroscopy (FTIR) results present band spectra characteristic of —OH stretching vibration in the cellulose of the fibre material. The absorption bands of the spectra are attributed to the presence of stretching vibration of C=O group mostly found in the form of hemicelluloses and lignin structure in the fibre. Upon examination of the test specimens produced through compression moulding technique, it was found that the addition of OPF (filler) into rHDPE (matrix) increased the composites' water absorption rate linearly for the first 16 days of exposure to the water environment. Stability was achieved for all the materials after this period. Thermal studies of the various compositions (OPF/rHDPE: 5/95, 10/90, 15/85, 20/80 and 25/75) using derivative thermogravimetric analysis (DTGA) showed two main degradation peaks at 490 °C and 380 °C. The mechanical study revealed that the composite with 20 wt% filler contents was the most eco-friendly and had the best mechanical properties while that with 25 wt% was the most thermally stable. This material was thermally stable up to approximately 330 °C. Microstructure examination of the different components of the composites further explains the reason for good physical and mechanical strength of the sample with 20 wt% filler. It can, therefore, be inferred from the results of the various analyses conducted that OPF is a good reinforcing phase for rHDPE and a potential material for construction and automotive industries.

© 2017 Karabuk University. Publishing services by Elsevier B.V. This is an open access article under the CC BY-NC-ND license (http://creativecommons.org/licenses/by-nc-nd/4.0/).

1. Introduction

A composite can be described as a structural material made up of two or more constituents that are combined at macroscopic level and are not soluble in each other [2]. While one constituent is called the reinforcing phase and may be in the form of fibres, particulates or flakes, the other constituent in which the reinforcing phase is embedded is called the matrix phase and is generally continuous [18]. There are naturally occurring composites like wood, where the lignin matrix is reinforced with cellulose fibres and bones in which soft collagen is reinforced with bone-salt plates made of calcium and phosphate ions [28]. Advanced composites are traditionally used in the aerospace and other high-tech industries are also in existence. They have high-performance reinforcements of a thin diameter epoxy in aluminium matrix [12]. These have also found applications for commercial industries worldwide.

The demands of today's advanced technologies require more than what monolithic metals and their alloys have to offer. It combines several materials to meet up with the performance requirements for the purpose of engineering applications [31,7]. For load-bearing applications, natural fibres are often mixed with polymers or precursor resins in order to increase stiffness, strength, and toughness. These enhancements depend on filler diameter, aspect ratio, alignment, dispersion and interfacial interaction [4,5,8]. For instance, engineers are continuously searching for ways of

---

* Corresponding author at: Nanotechnology Research Group, Centre for Genetic Engineering and Biotechnology, Federal University of Technology, P. M. B. 65, Minna, Nigeria.
   E-mail address: medupin.pg11723@st.futminna.edu.ng (R.O. Medupin).
   Peer review under responsibility of Karabuk University.

lowering the overall mass of the aircraft without decreasing the stiffness and strength of its components. This can be achieved only by replacing conventional metal alloys with composite materials. Although the initial composite's cost is high, the reduction in the number of parts in an assembly and fuel efficiency arising from light weight compensates for the initial cost. With fuel expenses consuming about 25% of the total operating costs of commercial airlines, reducing 0.453 kg of mass in a commercial aircraft can save up to 1360 l of fuel annually [12].

The advantages of using natural fibres in composites include light weight, high quality, low cost, annual renewability, good mechanical properties, reduced energy consumption and environmental friendliness [34]. Armin and Alan [3] reported that natural fibres which have high strength and modulus with good adhesion and uniform dispersion can impart better mechanical properties to the host polymer in order to obtain composites with better properties than those of the unfilled polymer. A coupling agent reduces the surface tension of the hydrophilic wood fibres to a level close to that of the molten polymer [21]. Therefore, wetting and adhesion are improved through diffusion and mechanical interlocking between the two entities. Catto et al. [9] and Ndiaye et al [24] addressed the problem of compatibility between wood reinforcement and polymer host matrix. According to their reports, wood fibres will not ordinarily adhere suitably to the polymer matrix because they are primarily incompatible. The introduction of a compatibilizer (sodium hydroxide, in this case) will enhance matrix-fibre adherence, and hence composite properties.

Oil palm fibre (OPF) is popular for its usage as alternative energy source. It is available in large quantity in Nigeria as the 5th largest producer of palm oil in the world, generating a significant amount of oil palm waste [11]. Rather than being a boost to the economy, this has, in no small measure, contributed to environmental pollution experienced in Africa. Oil palm waste is often used in the rural areas for cooking; hence the need to redirect this low-level utilisation to a better, safer and more profitable use. Zuhri et al. [35] reported that reinforcing rubber with short OPFs imparts good strength and stiffness to soft as well as tough rubber matrices. In a similar work, Redwan et al. [27] found that impact strength is adversely affected by the incorporation of empty fibre bunches (EFBs) into modified and unmodified unplasticized polyvinyl chloride (PVC-U). In a similar study, Khairiah and Khairul [13] reported that the highest hardness as well as better impact and flexural strength are imparted on EFB/polyurethane (PU) composite with a ratio of 35:65. They also found that better adhesion between PU matrix and EFB fibres results in better water resistance.

The objective of the study is to develop biodegradable composites from OPF and rHDPE; provide viable test data that will help in tailoring their applications appropriately as candidates for application in both construction and automotive industries.

2. Materials and methods

2.1. Materials

Recycled high-density polyethylene (rHDPE) was collected from the Federal Polytechnic Bida, Nigeria. Oil palm fibres were sourced from a local oil mill in Bida local government area of Niger State, Nigeria. Sodium hydroxide of analytical grade with percentage purity of 99.99% and manufactured by Burgoyne & Co. Mumbai, India was supplied by Panlac Nig. Ltd, Minna, Nigeria. The distilled water used throughout the experiment was produced at the Centre for Genetic Engineering and Biotechnology, Federal University of Technology, Minna, Nigeria.

2.2. Methodology

The rHDPE was thoroughly washed with clean water followed by rinsing with distilled water and dried at room temperature for 24 h. Because of the crude method used by the local millers for oil extraction, it was noticed that the OPFs still contained some oil that must be extracted before usage. In order to remove the residual oil, therefore, the fibres were boiled for three hours and the oil was removed to the barest minimum, dried and pretreated with superheated steam. In order to enhance their interfacial interaction with the host polymer matrix, the fibres were soaked in 2 M concentration NaOH for 24 h and then washed thoroughly until its pH value became neutral. The fibres were again dried in air and milled to smaller particles after which sieve analysis was carried out to separate the particles into sizes. Size 150 μm sieve was used in this study. The composites were compounded using compression moulding manufacturing technique. The superheated steam-treated oil palm fibres (0, 5, 10, 15, 20 and 25 wt%) were used to reinforce recycled high-density polyethylene (rHDPE). The compounding followed the procedure described by Nemati et al. [25].

Using counter-rotating two-roll open mill (5183, USA) with rotor speeds for the front and rear rolls adjusted to 30 rpm and 18 rpm respectively and working distance of 300 mm, the rHDPE was masticated for 4 mins and OPF of different wt%, as stated above, were introduced into the mix. Mixing continued for additional 6 mins to ensure homogeneous distribution of the treated fillers. The fully masticated and mixed composite was then put in a pre-heated mould fabricated for the purpose of the study; it was then cured at 100 °C for 10 mins in an electrically heated hydraulic press. Thereafter, the specimen was cooled under pressure (3 bar) at room temperature and neatly packed for analyses.

2.3. Water absorption

The composite samples with dimensions, 50 mm long, 10 mm wide and 3 mm thick, were dried in the oven at 70 °C for 45 mins, until constant weights were achieved. They were then immersed in distilled water at room temperature for a period of 1200 h according to ASTM D570. At predetermined interval, specimens were removed, dried, weighed and returned to the water. Percentage of moisture content was calculated according to Eq. (1) [19].

$$M_n = \frac{W_w - W_d}{W_w} \times 100 \tag{1}$$

where M_n is the moisture content (%) of the different samples, W_w is the wet weight of the samples and W_d is the final weight of the sample after a defined period of 240 h.

2.4. Thermogravimetric analysis

Thermal decomposition was observed in terms of global mass loss by using a TA Instruments, TGA Q50 thermogravimetric analyser. To determine the thermal stability of the samples, argon gas was allowed to flow through the system at the rate of 20 ml/min and at a pressure of 3 bar. 10 mg of the sample was evenly and loosely distributed in an open sample pan of 7.4 mm diameter and 4.2 mm deep. The temperature was set between 25 ± 3 °C and 900 °C at a heating rate of 20 °C/min. The data and corresponding TGA curve was then generated.

2.5. Scanning electron microscopy

Phenom ProX SEM machine was used to take the microstructure images of the samples at 1500x magnification and an accelerating voltage of 15 kV. Fractured samples were used to study fibre distribution in the composites. About 1.0 g of the composite sample was

mounted on aluminium stubs with colloidal graphite as the mounting media after which the sample was coated with carbon. This was then treated with gold palladium deposition to make the surface of the composite conductive. The coated sample was then examined under the microscope.

2.6. Fourier Transform Infrared Spectroscopy

Fourier Transform Infrared (FTIR) Spectroscopy analysis was conducted using Shimadzu instrument. A small part was taken from the different composites and pelletized. A few milligrams of the samples were mixed with 0.5 g potassium bromide (KBr). The pellet was placed between interferometer and detector in the sample holder of the spectroscope. The sample was then placed in the FTIR spectroscopy with red light source generating wavelength from 4000 to 400 cm^{-1}. Infrared spectra generated were recorded in the absorption mode and presented in Fig. 7.

2.7. Mechanical tests

Tensile test was carried out using universal testing machine (Monsanto Tensometer model number 9875) under ambient conditions according to ASTM D638. Dumb-bell shaped specimens were used for the tests.

A 45° notch was machined into each of the samples of geometry 80 mm length, 12 mm width and 6 mm thick. The test was carried out using Charpy impact testing machine and according to ASTM D6110-06 standard at a velocity of 3.5 m/s, a 150° angle and a 0.5 J hammer. Running at ambient temperature with a fixed weight of 6.45 kg, the impactor was adjusted to provide a velocity of 3 m/s and impact energy of 12 J. The impact strength of each sample was read directly from the scale and recorded.

INDENTEC universal hardness testing machine with model number 8187-5LKV(B) was used for the hardness test of the samples at room temperature. Cubical samples were obtained from the composites and tested for hardness.

3. Results and discussion

3.1. Water absorption

Water absorption analysis shows a uniform water uptake in the first 16 days before becoming relatively stable as depicted in its near-zero gradients after 400 h of being immersed in water (Fig. 1). Cellulose and hemicelluloses were reported to be most responsib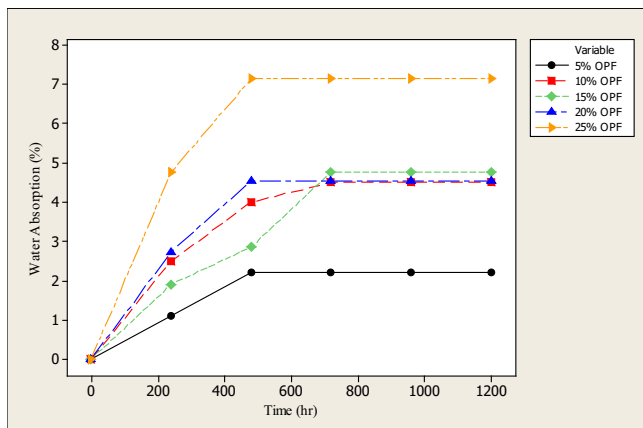le for high water absorption in organic fillers. As filler content increased, the cellulose also increased and hence, increase in water absorption [22]. The 0.5% water absorption rate for the first 16 days can be attributed to good filler dispersion in the matrix during production. Judging from the absorption-time curve presented in Fig. 1, water uptake increases with increase in filler content. Although the results presented indicate that the composite with the least filler content is the most stable in a humid environment, with maximum water uptake of approximately 2% at a soaking time of 1400 h. The composites with 10–15 wt% filler were also considered to be stable with maximum water uptake in the ranges of 4.5–4.8% at the same soaking time. It is also worth mentioning that water uptake increased with increase in filler content as a result of the numerous hydroxyl groups (–OH) which are normally there to interact with water molecules by hydrogen bonding [16]. In spite of the higher water uptake noticed with increase in filler content, the materials are still considered as durable engineering material based on literature values reported by Alomayri et al. [1].

3.2. Thermogravimetric analysis

TGA measures the weight change of a sample as a function of temperature in the scanning mode or as a function of time in the isothermal mode in a controlled atmosphere. Under specified condition, TGA is used to characterise the degradation and thermal stability of materials [6]. Thermal stability of the neat rHDPE and composites produced was tested and Figs. 2 to 7 show the TGA results generated on OPF reinforced rHDPE polymer composite with varying filler contents. The plots show the percentage mass as a function of temperature for the unfilled and polymer composite under an argon purge. The principal events from the thermographs in Figs. 2–7 are listed in Table 1. rHDPE/OPF-5 undergoes thermal degradation with a total mass loss of about 96%. When subjected to the furnace temperature between 30 and 900 °C, the composite initially lost about 4% moisture. This was followed immediately by matrix degradation between 200 °C and 502 °C. Between 502 °C and 640 °C, the filler phase decomposed with other volatiles. There was about 2.4% of inert residue remaining after the thermal degradation.

From Table 1, it is clear that thermal stability is improved with increase in organic filler content. The thermal degradation patterns of the composites revealed that the neat matrix is less thermally stable than the composites except in the case of sample rHDPE/OPF-15 where the peak temperature (T_p) was 381.0 °C (T_p for neat matrix is 413 °C). The unexpected fall in rHDPE/OPF-15 could be
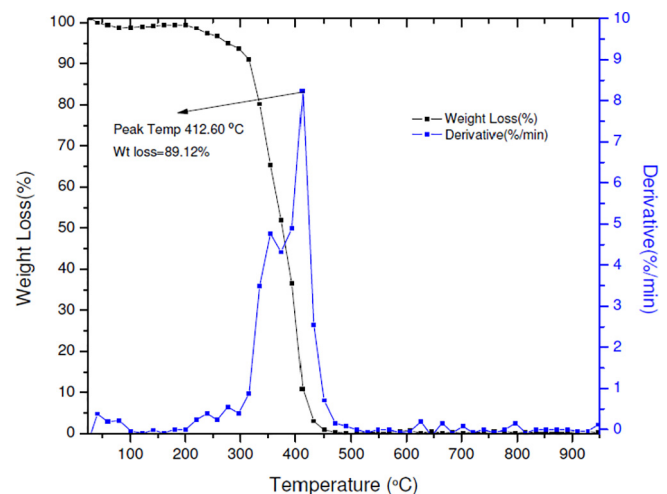

Fig. 1. Absorption – Time Curve of composites with Varying wt% reinforcement.

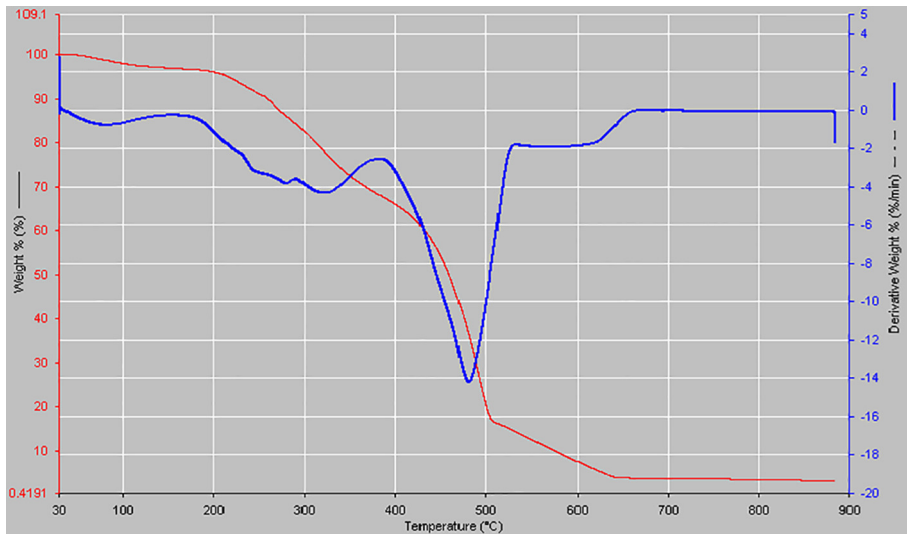**Fig. 2.** TGA/DTG thermograph for rHDPE/OPF-0.

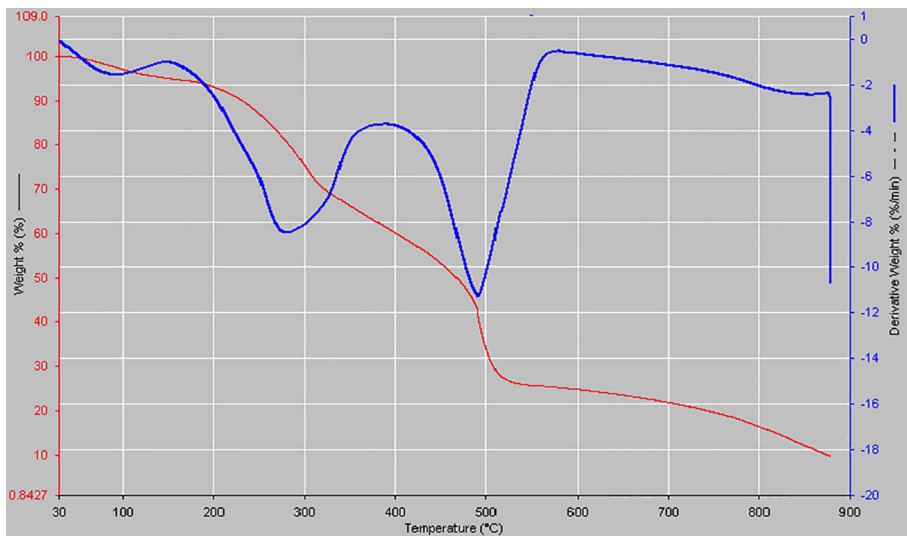**Fig. 3.** TGA/DTG thermograph for rHDPE/OPF-5.

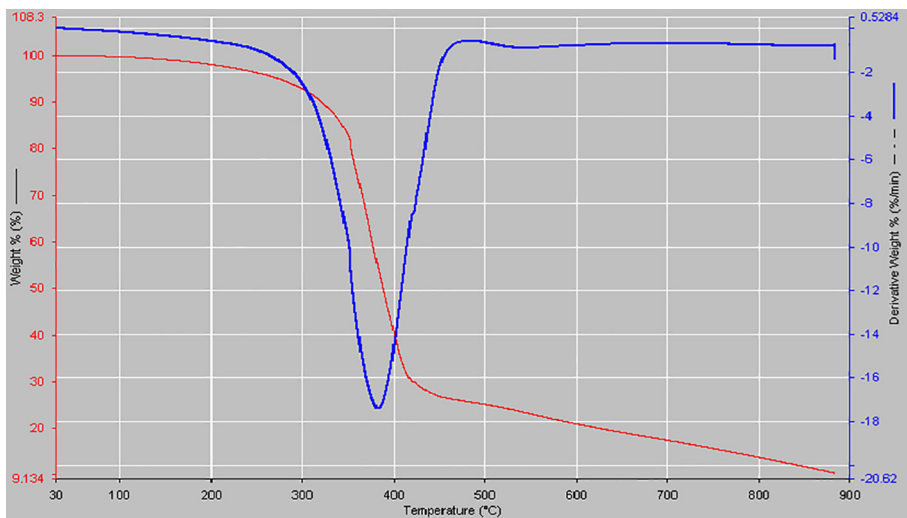**Fig. 4.** TGA/DTG thermograph for rHDPE/OPF-10.

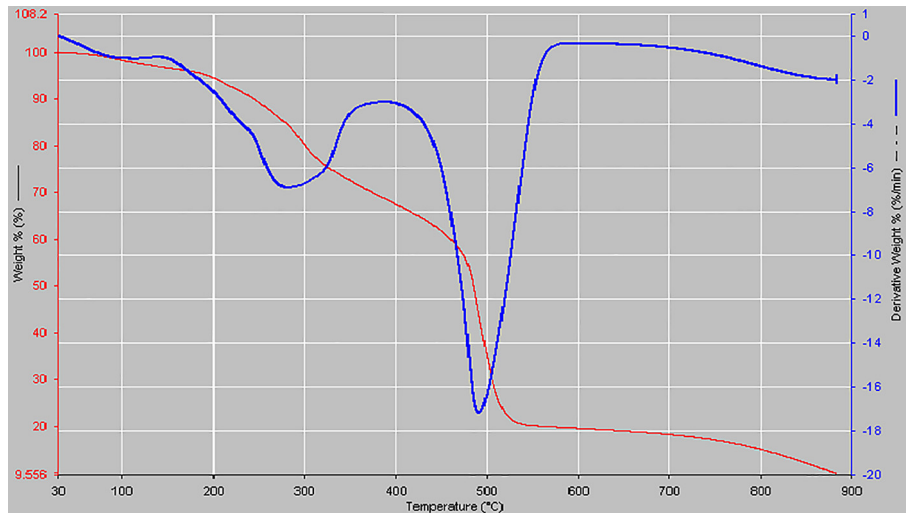**Fig. 5.** TGA/DTG thermograph for rHDPE/OPF-15.

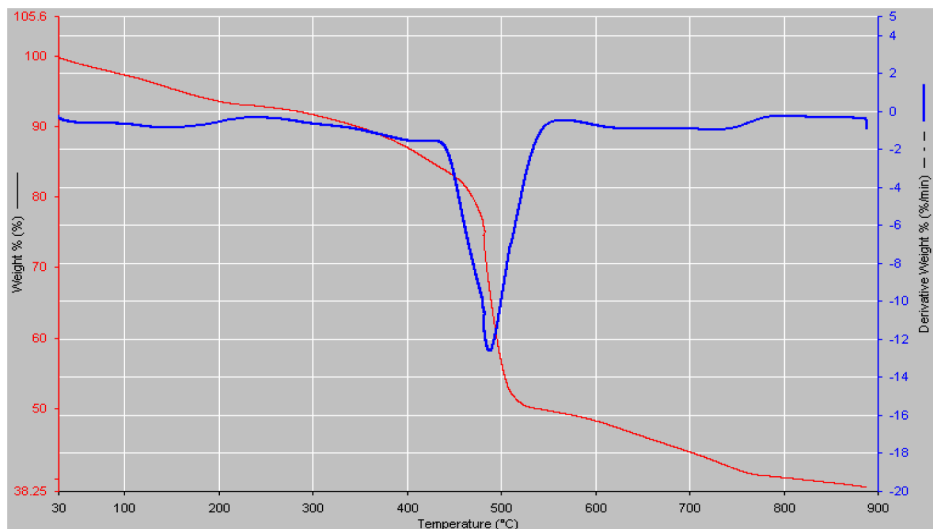**Fig. 6.** TGA/DTG thermograph for rHDPE/OPF-20.

Fig. 7. TGA/DTG thermograph for rHDPE/OPF-25.

Table 1
TGA parameters of Different Composition of rHDPE/OPF composites.

Sample	Peak Temperature, T_p (°C)	$T_{50\%}$ (°C)	Onset Temperature, T_{onset} (°C)	Degradation Temperature (°C)
rHDPE/OPF-0	413.0	385.0	290.0	200.0–450.0
rHDPE/OPF-5	475.0	459.0	225.0	200.0–638.0
rHDPE/OPF-10	491.0	469.0	215.0	198.0–700.0
rHDPE/OPF-15	381.0	391.0	335.0	240.0–600.0
rHDPE/OPF-20	491.0	480.0	233.0	200.0–650.0
rHDPE/OPF-25	492.0	520.0	300.0	250.0–763.0

attributed to inability to attain homogeneous distribution of filler in the matrix. The composites with lower fibre content degrade faster with a single degradation peak at temperature ranges reported in Table 1. Two degradation peaks are observed in Figs. 3, 4 and 6; the small peaks representing the degradation of the OPF contained in the composites; occurring around 325 °C, 275 °C, and 278 °C respectively while the main peaks are 475 °C, 491 °C and 491 °C. On the other hand, Fig. 7 has a single degradation peak of 492 °C as clearly stated in Table 1.

At 5 wt% reinforcement, T_p of the composite was 475 °C, a value that later increased at 10 wt% reinforcement. The amount of OPF present was initially small, indicating a possibility that the thermal properties of the HDPE predominated over that of the OPF. This masked the influence of the OPF on the thermal stability of the composites, resulting in the observed trend. However, as the fibre content increased to 15 wt%, thermal stability was noticed to drop significantly against the expected trend. T_p decreased reasonably as a result of the lower thermal stability of OPF when compared to

HDPE [33]. Composites containing 20 wt% and 25 wt% OPF exhibited increase in thermal stability possibly because of the higher amount of filler content. In addition, onset temperature (T_{onset}), peak temperature (T_p), and the temperature at which 50% mass of the composites degraded $(T_{50\%})$ increased with filler content in the composites (Table 1).

It can be concluded from TGA analysis that the composite materials were generally thermally stable. However, when allowed to progress to completion, pyrolysis resulted in the complete conversion of polyethylene to gaseous hydrocarbons with no char produced [29]. Such condition can rarely be encountered under normal service conditions. Therefore, judging from the T_p, the T_{onset} and the degradation temperature range obtained for the composites (Table 1), it is evident that the composites will withstand temperatures expected in service life.

3.3. Fourier transform infra-red spectroscopy

The results of the FTIR analysis are presented in Fig. 8. Generally, the regions of the spectra are divided into the functional group region (4000–1300 cm^{-1}) and the fingerprint region (1300–650 cm^{-1}).

The band spectra between the absorption peak of 3974 cm^{-1} and 3000 cm^{-1} are characteristic features of —OH stretching vibration in the cellulose of fibre reinforcement used during the composite production. The absorption peaks around 3974 cm^{-1} and 3000 cm^{-1} for all the composites showed varied intensity and also a shift in the wavenumber due to the variation of fibre percentage in the mixture of the rHDPE binder. This result is in close agreement with the report of Kondo [15]. Basically, the absorption band is around 1720 cm^{-1} in 10 wt% fibre reinforced composite, 1719 cm^{-1} in 20 wt% fibre reinforced composite, and 1781 cm^{-1} in 25 wt% fibre reinforced composite are attributed to the presence of stretching vibration of C=O group [14]. Group C=O were mainly found in the components of the fibre in the form of hemicellulose and lignin structure. This is in agreement with the report Siwatt Pongpiachan [30]. Also, there was a disappearance of the C=O

group band in the 5 wt% fibre reinforced composite. This disappearance might be as a result of complete engulfment of the fillers by rHDPE matrix. Furthermore, the band frequency at 733 cm^{-1} in sample b and c, as indicated in Fig. 8, shows the presence of =C—H bound stretching group present in the composite.

This =C—H functional group was found to shift to the right in sample a, d and e to around 710 cm^{-1}. Also, the band wavenumbers at 1350 cm^{-1}, 1368 cm^{-1}, 1352 cm^{-1}, 1379 cm^{-1} and 1352 cm^{-1} in sample a, b, c, d and e respectively were characteristic absorption frequencies of C—H bending vibration with slight variation in frequency number due to the varied percentage composition makeup of the polymer composites. Meanwhile, the presence of C=C aromatic symmetrical stretching bond were observed at 1567 cm^{-1}, 1567 cm^{-1}, 1565 cm^{-1} and 1575 cm^{-1} in sample b, c, d and e respectively. The disappearance of the absorption peak in sample a is related to the presence of lower percentage of fibre in the composite. Also, C—C, C—OH, C—H ring and side group vibrations were all observed throughout the polymer composites at adsorption peaks of 1024 cm^{-1}, 1012 cm^{-1}, 1010 cm^{-1}, 1015 cm^{-1} and 1036 cm^{-1} for sample a, b, c, d and e respectively with a dislocation at sample e due to the high level of fibre present in it.

3.4. Mechanical properties

The tensile strength of OPF reinforced polymer composites as a function of oil palm content is shown in Fig. 9. The tensile strength increased with increasing filler loading relative to the pure matrix [32]. This implies that as OPF content increased, good wetting of the fibres are still guaranteed as there was less fibre-to-fibre contact. During testing, therefore, especially in the tensile mode, very few unwetted fibres could become stress concentration areas which eventually accounted for early failures and low strength [17].

The results presented in Fig. 10, show that the hardness value of the composites increased with increased filler content. This is in agreement with earlier studies in which natural fillers were used as reinforcing medium in a polymeric host matrix [23]. What this
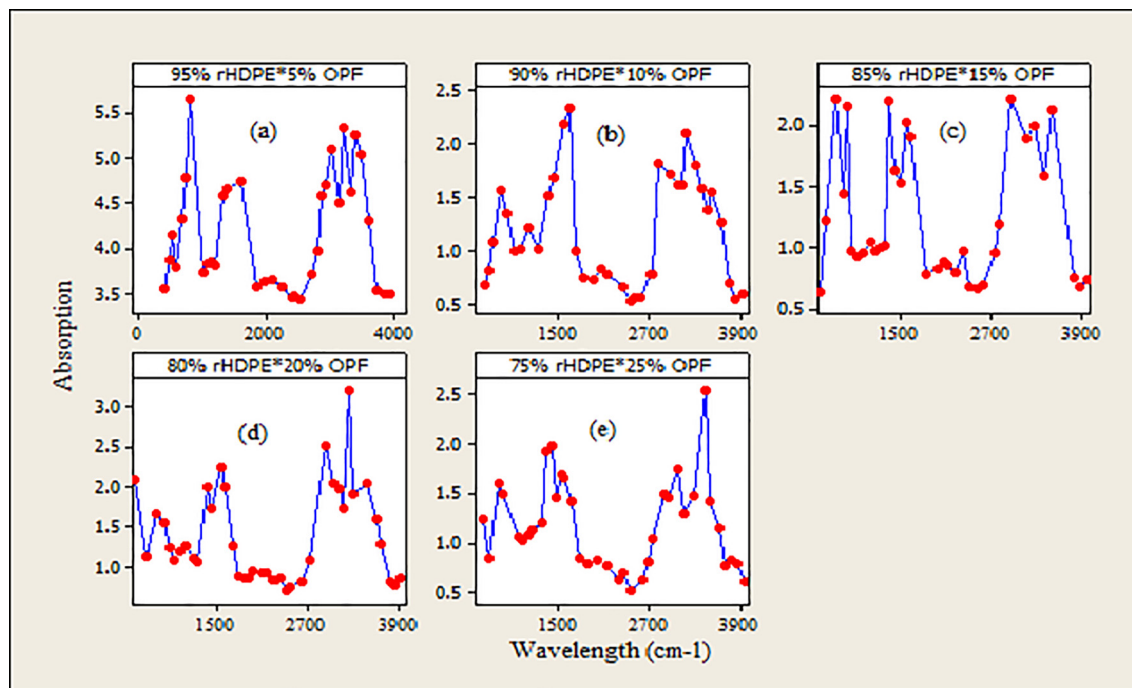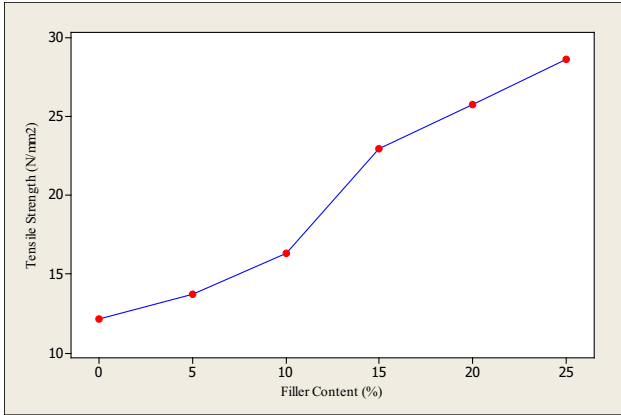

Fig. 8. FTIR Spectra of the Composites.

Fig. 9. Variation of Tensile Strength with OPF reinforcement.
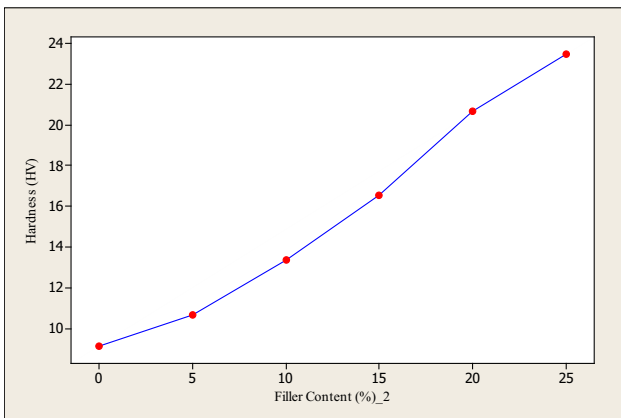

Fig. 10. Variation of Hardness with OPF reinforcement.

implies, in principle, is that the presence of less ductile fillers helped to achieve balance between the two major components of the composite by imposing brittleness on the matrix [10]. The improvement in the hardness values can be attributed to the intrinsic high strength and Young's modulus of the OPF [20]. As reinforcement increases, the composites tend to become stiffer and hence harder, as shown in Fig. 10 [21].

Plastic materials are normally exposed to impact encounters that could lead to failure. It is, therefore, important to know what maximum loads they can sustain without failing. It can be seen in
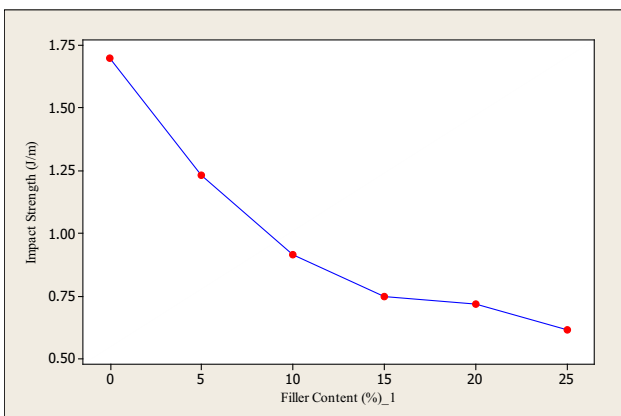
Fig. 11 that impact strength decreases as the filler content increases. This is in agreement with the report of Zuhri et al. (2009) in which OPFs were used as reinforcing fillers in rubber.

Tensile modulus graph is presented in Fig. 12. The trend is similar to earlier reports by Medupin and Abubakre, (2015) and Pickering et al. [26] as it increased with increase in filler content. On the other hand, impact strength and deflection reported in Figs. 11 and 13 decreased with increase in filler loading.

3.5. Scanning electron microscopy microstructures of composites

The morphologies of the neat polymer and the developed composites are presented in Plates 1–6. It can be inferred from the micrographs that the bulk of failure likely occurred as a result of fibre pull out from the matrix or inhomogeneous distribution of the fibres, as shown in Plates 3 and 5. This could possibly result from inadequate composite interfacial interaction during mechanical mixing. It can also be asserted that the failure experienced during testing could be as a result of inadequate wetting of the surface areas of filler materials by the matrix during compounding and hence, fibre pull-out and eventual failure of the composites were inevitable[17]. But by visual observation of the microstructure, except for composites with 10 wt% and 20 wt% fibres content, the compounding was reasonably acceptable. The high water resistance capacity of the samples also verified the fact that the adherence of the constituent parts was adequate.

Pockets of filler agglomerates was spotted in the micrographs (except in the case of neat polymer in Plate 1) indicating that there will be hindrances to load transmission in the composites during
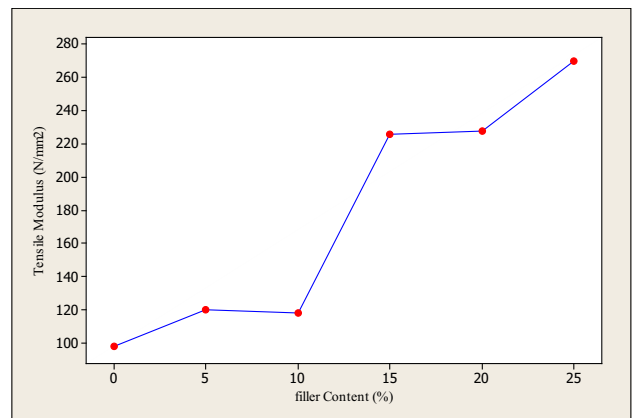

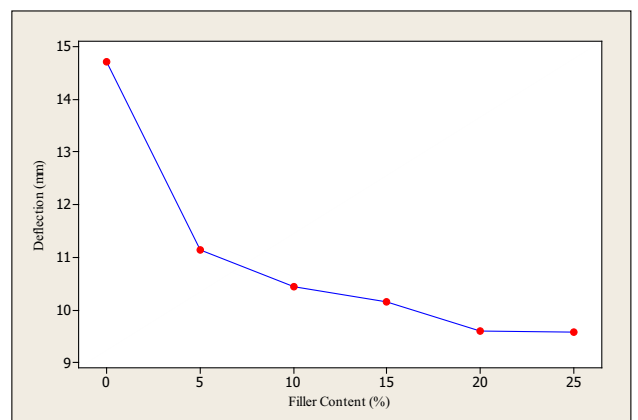**Fig. 12.** Variation of Tensile modulus with OPF reinforcement.

Fig. 11. Variation of Impact Strength with OPF reinforcement.

Fig. 13. Variation of Deflection with OPF reinforcement.
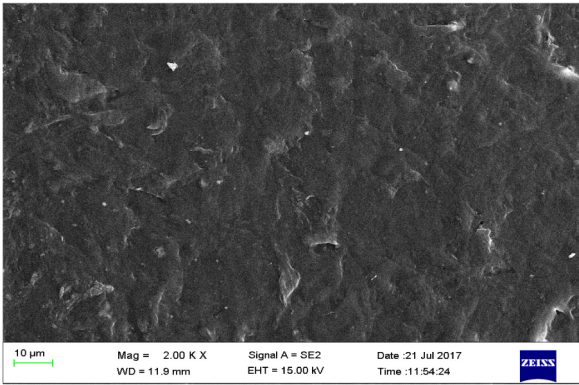
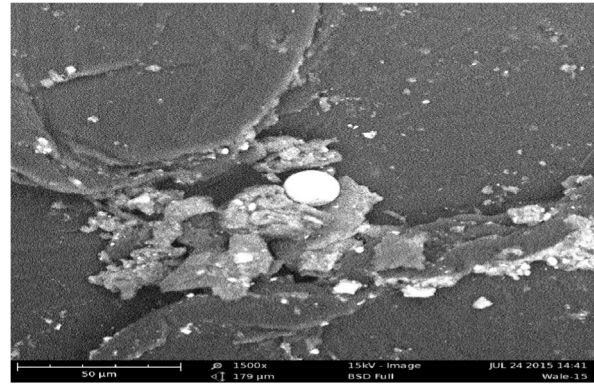**Plate 1.** 0 wt% OPF in rHDPE.

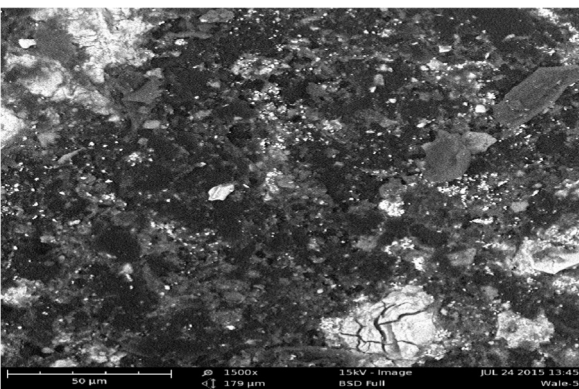**Plate 4.** 15 wt% OPF in rHDPE.

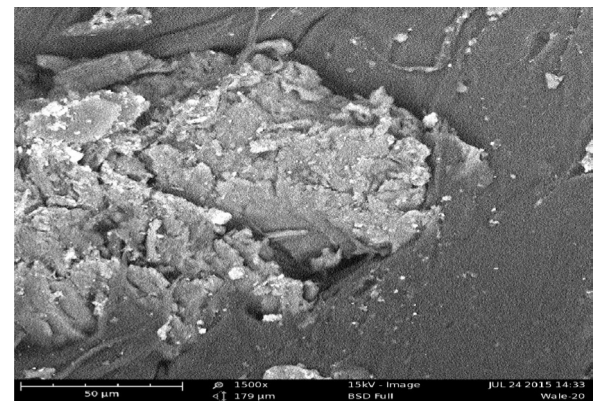**Plate 2.** 5 wt% OPF in rHDPE.

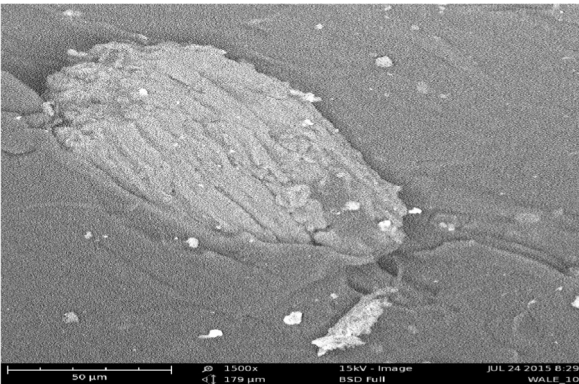**Plate 5.** 20 wt% OPF in rHDPE.
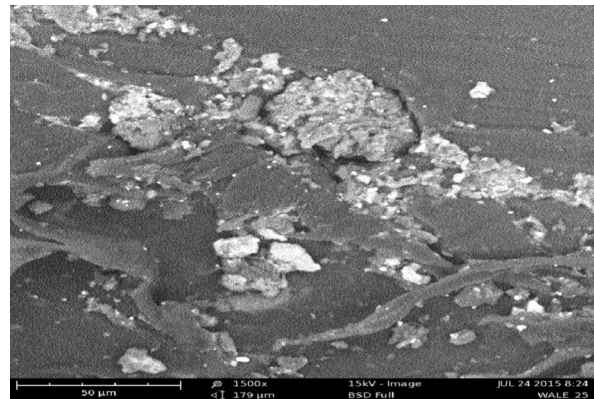

Plate 3. 10 wt% OPF in rHDPE.

Plate 6. 25 wt% OPF in rHDPE.

tensile load or compressive force application. The fillers, expected to serve as the medium through which loads were transferred, when not uniformly distributed, hampered the flow and hence caused early material failure.

4. Conclusion

The results presented in this study showed that thermal analysis and physico-mechanical analysis are reliable methods to study environmental, thermal stability, physical and mechanical behaviours of natural fibres reinforced polymer composite for structural application. Areas of possible application include flooring, stairs, mallet and other such applications. Five different filler ratios were studied under the same conditions and it was found that the suitability of the composites for structural application was enhanced by the addition of fillers with 20 wt% filler content being the most environmentally, mechanically and thermally stable of the five composite materials produced with good mechanical properties. This material offers a good option for structural application and is thermally stable up to about 330 °C. Microstructure examination of the different compositions of the composites further explains the reason behind good physical and mechanical strength of the sample with 20 wt% filler. This study is expected to be taken to

the next level of investigating the viscoelastic behaviours of the materials for applications other than structural.

Acknowledgements

References

[1] T. Alomayri, H. Assaedi, F.U.A. Shaikh, I.M. Low, Effect of water absorption on the mechanical properties of cotton fabric-reinforced geopolymer composites, J. Asian Ceram. Soc. 2 (3) (2014) 223–230.

[2] A.O. Ameh, M.T. Isa, I. Sanusi, Effect of particle size and concentration on the mechanical properties of polyester/date palm seed particulate composite, Leonardo Electron. J. Practices Technol. 26 (2015) 56–78.

[3] T. Armin, R.D. Alan, The influence of fibre length and damage on the mechanical performance of polypropylene/wood pulp composites, Compos.: Part A 46 (2013) 45–52.

[4] R. Atif, F. Inam, Reasons and remedies for the agglomeration of multilayered graphene and carbon nanotubes in polymer, Beilstein J. Nanotechnol. 7 (2016) 1174–1196, https://doi.org/10.3762/bjnano.7.109.

[5] M. Bahttacharya, Polymer nanocomposites – a comparison between carbon nanotubes, grapheme and clay as nanofillers, Materials 9 (262) (2016) 1–35, https://doi.org/10.3390/ma9040262.

[6] R. Banat, M.M. Fares, Thermo-gravimetric stability of high density polyethylene composite filled with olive shell flour, Am. J. Polym. Sci. 5 (3) (2015) 65–74, https://doi.org/10.5923/j.ajps.20150503.02.

[7] M.O. Bodunrin, K.K. Alaneme, L.H. Chown, Aluminium matrix hybrid composite: a review of reinforcement philosophies; mechanical, Corrosion and tribological characteristics, J. Mater. Res. Technol. 4 (4) (2015) 434–445, https://doi.org/10.1016/j.jmrt.2015.05-003.

[8] L. Bokobza, Mechanical and electrical properties of elastomer nanocomposites based on different carbon nanomaterials, J. Carbon Res. 3 (10) (2017) 1–22, https://doi.org/10.3390/c3020010.

[9] A.L. Catto, B.V. Stefani, V.F. Ribeiro, R.M.C. Santana, Influence of coupling agent in compatibility of post-consumer HDPE in thermoplastic composites reinforced with eucalyptus fiber, Mater. Res. 7 (2014) 203–209. org/10.1590/S1516-14392014005000036.

[10] M. Chinomso, C.M. Ewulonu, I.O. Igwe, Properties of oil palm empty fruit bunch fibre filled high density polyethylene, Int. J. Eng. Technol. 3 (6) (2012) 458–471.

[11] Green Palm Sustainability, Top Palm Producing Nations, January – December, 2015.

[12] A.K. Kaw, Mechanics of Composite Materials, 2nd ed., Taylor & Francis Group, CRC Press, New York, 2006.

[13] B. Khairiah, A.M.A. Khairul, Biocomposites from oil palm resources, J. Oil Palm Res. (2006) 103–113.

[14] S. Khan, A.M. Zain, T. Murugesan, Identification and characterization by FTIR, TGA and UV/Vis spectroscopy of phenilic compound (Gallic Acid) from Nephelium Lappaceum leaves for medical use, J. Appl. Sci. Agric. 10 (5) (2015) 189–195.

[15] T. Kondo, Hydrogen bonds in cellulose and cellulose derivatives, in: Dumitriu S (Ed.), ISBN 3-540-37102-8, New York, USA, 2005.

[16] B. Kord, Effect of wood flour content on the hardness and water uptake of thermoplastic polymer composites, World Appl. Sci. J. 12 (9) (2011) 1632–1634.

[17] R.A. Lafia-Araga, A. Hassan, R. Yahya, N.A. Rahman, P.R. Hornsby, J. Heidarian, Thermal and mechanical properties of treated and untreated Red Balau (Shorea dipterocarpaceae)/LDPE composites, J. Reinf. Plast. Compos. 31 (4) (2012) 215–224.

[18] G. Markovic, O. Veljkovic, M. Marinovic-Cincovic, V. Jovanovic, S. Samarzija-Jovanovic, J. Budinski-Simendic, Composites based on waste rubber powder and rubber blends: BR/CSM, Compos.: Part B 45 (2013) 178–184.

[19] B. Masseteau, F. Michaud, M. Irle, A. Roy, G. Alise, An evaluation of the effects of moisture content on the modulus of elasticity of a unidirectional flax fiber composite, Composites 60 (2014) 32–37.

[20] R.O. Medupin, O.K. Abubakre, Effect of wood fibre characteristics on the properties of wood polymer composites, J. Multi. Sci. Technol. 2 (1) (2015) 101–105.

[21] L. Mohammed, M.N.M. Ansari, G. Pau, M. Jawaid, M.S. Islam, A review on natural fibre reinforced polymer composite and its applications, Int. J. Polym. Sci. 2015 (2015) 1–15. org/10.1155/2015/243947.

[22] E. Munoz, A. Garcia-Manrique, Water absorption behaviour and its effect on the mechanical properties of flax fibre reinforced bioepoxy composite, Int. J. Polym. Sci. 2015 (2015) 1–10, https://doi.org/10.1155/2015/390275.

[23] S. Navaneethakrishnan, A. Athijayamani, Mechanical properties and absorption behaviour of CSP filled roselle fibre reinforced hybrid composites, J. Materi. Env. Sci. 7 (5) (2016) 1674–1680.

[24] D. Ndiaye, E. Fanton, S. Morlat-Therias, L. Vidal, A. Tidjani, J. Gardette, Durability of wood polymer composites: Part 1. Influence of wood on the photochemical properties, J. Compos. Sci. Technol. 68 (2008) 2779–2784.

[25] M. Nemati, H. Khademieslam, M. Talaiepour, I. Ghasemi, B. Bazyar, Investigation on the Mechanical properties of nanocomposite based on wood flour/ recycle polystyrene and nanoclay, J. Basic. Appl. Sci. Res. 3 (3) (2013) 688–692.

[26] K.L. Pickering, M.G. Aruan Efendy, T.M. Le, A review of recent developments in natural fibre composite, Part A: Appl. Sci. Manuf. 83 (2016) 98–112, https://doi.org/10.1016/j.compositesa. 2015.08.038.

[27] A. Redwan, K.H. Badri, A. Baharum, A urethane block copolymer as binder for fire-resist palm-based fibreboard, Polym. Polym. Compos. 24 (9) (2016) 681–686.

[28] M. Sadat-Shojai, M.T. Khorasani, E. Dinpanah-Khoshdargi, A. Jamshidi, Synthesis methods for nanosized hydroxyapatite with diverse structures, Acta Biomater. 9 (2013) 7591–7626, https://doi.org/10.1016/j.actbio.2013.04.012.

[29] V.S. Sikarwar, M. Zhao, P. Clough, J. Yao, X. Zhong, M.Z. Memon, N. Shah, E.J. Anthony, P.S. Fennell, An overview of advances in biomass gasification, Energy Environ. Sci. 9 (2016) 2939–2977, https://doi.org/10.1039/c6ee00935b.

[30] Siwatt Pongpiachan, FTIR spectra of organic functional group compositions in $PM_{2.5}$ collected at Chiang-Mai city, Thailand during the haze episode in March 2012, J. Appl. Sci. 14 (2014) 2967–2977.

[31] S.C. Tjong, Processing and deformation characteristics of metal reinforced with ceramic nanoparticles, Nanocryst. Mater. 2 (2014) 269–304, https://doi.org/10.1016/B978-0-12-407796-6-00008-7.

[32] R.M. Wang, S.R. Zheng, Y.P. Zheng, Polymer matrix composites and technology, Woodhead Publishing Limited (Science Press), Cambridge, UK, 2011.

[33] L. Xie, T. Grueneberg, L. Steuernagel, G. Ziegmann, H. Militz, Influence of particle concentration and type on flow, thermal, and mechanical poperties of wod-plypropylene composites, J. Reinf. Plast. Compos. 29 (13) (2010) 1940–1951.

[34] T.H. Ziaei, F. Rafiee, H. Khademi-eslam, M. Pourbakhsh, Thermo-chemical Evaluation of wood plastic nanocomposites, 463–464, Advanced Materials Research, 2012.

[35] M.Y.M. Zuhri, S.M. Sapuan, N. Ismail, Oil palm fibre reinforced polymer composites: a review, Progress Rubber Plast. Recycl. Technol. 25 (4) (2009) 233–246.